This is a repository copy of *System optimal routing and distribution of benefits on national road networks*.

White Rose Research Online URL for this paper:
https://eprints.whiterose.ac.uk/221863/

Version: Published Version

World Conference on Transport Research - WCTR 2023 Montreal 17-21 July 2023

System Optimal Routing and Distribution of Benefits on National Road Networks

Alexander Roocroft[a,b], Giuliano Punzo[a], Muhamad Azfar Ramli[b]

[a]Department of Automatic Control and Systems Engineering, University of Sheffield, Sheffield, United Kingdom
*[b]Institute of High Performance Computing, A*STAR, Singapore*

Abstract

Rerouting drivers from selfish route choices to system-optimal traffic patterns has the potential to improve the performance of existing infrastructure. Previous research has looked into assessing the potential of rerouting through the empirical price of anarchy, a measure of network efficiency. However, studies using real-world measurements have been limited by methodological accuracy and network size. Also, they have lacked understanding of the spatial distribution of benefits from rerouting and the relationship with marginal external cost road charges that can be used for implementation. In this article, we create an accurate data-driven traffic assignment model of England's Strategic Road Network. We use it to calculate the national price of anarchy, which is found to be almost 1 implying gains from rerouting at the national scale are minimal and smaller than in other studies. The results show the distribution of rerouting benefits varies strongly with different network zones and demand profiles. This did not match the distribution of marginal external cost charges. Some zones have noticeable benefits from rerouting although the overall network benefit is small, however, these zones do not coincide with where the largest road charges have to be applied for system-optimal rerouting. These results have implications for rerouting implementation.

Keywords: Strategic Road Network, Empirical Price of Anarchy, National Traffic Assignment.

1. Introduction

In many countries around the world road congestion continues to cost billions in economic losses each year, and this is predicted to rise (INRIX (2021)). Conventional approaches to traffic congestion reduction have been to build more roads and capacity. However, due to induced demand effects and increasing environmental costs this is not always effective or viable option (Hymel et al. (2010)). As an alternative to making physical changes to the network, potential improvements to congestion can be made from directing drivers to use the network more efficiently utilising intelligent

---

*Corresponding author.
E-mail address: aroocroft1@sheffield.ac.uk

transport systems such as connected autonomous vehicles and road-specific road charges (Zhang et al. (2018)). Drivers on the road seek to minimise their own selfish travel cost through their choice of route without considering the effect on the transport system overall. Their non-cooperative behaviour leads to emergence of Wardrop equilibrium patterns referred to as User-Equilibrium (UE), where no driver can improve their travel cost assuming the other drivers' routes are fixed (Youn et al. (2008)). The use of static Traffic Assignment (TA) models has been investigated as potential way to analyse traffic patterns and calculate System-Optimal (SO) routing that reduces global travel costs from UE by more efficient route allocation (Patriksson (2015)). The dimensionless metric of the Price of Anarchy (POA) metric is used to quantify the loss in performance from selfish UE routing compared to globally SO patterns (Zhang et al. (2018)).

Technological developments in traffic data collection have created opportunities to measure the cost of uncoordinated driving on large-scale real-world transportation systems. Different methodological approaches have been used to quantify the empirical POA (Table 1). Previous work using real-world measurements has been limited by the accuracy of the methods used for calculating the traffic patterns or restricted to smaller network sizes by the techniques used to create the static TA model (Monnot et al. (2017); Zhang et al. (2018)). Others have included additional synthetic data (Youn et al. (2008); De Grange et al. (2017)) that reduced empirical validity, or incorporated dynamic effects through micro-simulation that increased computational cost (Belov et al. (2022)). Currently such empirical POA research has not investigated in detail from a network perspective the distribution of benefits from large-scale rerouting and the relationship with marginal cost road charges. By investigating this it adds extra insight into how rerouting allocates the costs on a network, providing a greater comprehension of any practical implementation issues and the fairness of potential benefit distributions. These are essential for planners to understand how such schemes impact road users in different regions of networks.

Study	Model Type	Analysis Description	Network location/type	POA Range
Youn et al. (2008)	Synthetic demand in static TA	Demand varied on single O-D pair	Boston, New York and London	1.24 - 1.30
O'Hare et al. (2016)	Synthetic demand in static TA	Demand varied on different numbers of O-D pairs	Sioux Falls test network	1 - 1.1
De Grange et al. (2017)	Synthetic demand in static TA	Demand varied for reference matrices with alternative congestion function parameters	Santiago de Chile, Anaheim and Chicago	1.06 - 1.09
Monnot et al. (2017)	Individual commuter data without TA model	Acquired the SO routing via Google Directions and compared with recorded commuter routes	Singapore	1.11 - 1.22
Zhang et al. (2018)	Mobile phone data-driven static TA	Data-driven TA model used to calculate SO pattern for comparison with observed traffic	Eastern Massachusetts	1 - 2.3
Wu et al. (2021)	Synthetic demand in static TA	Number of O-D pairs varied when loading the network	Beijing	1
Belov et al. (2022)	Synthetic data in dynamic TA using micro-simulation	Varied the micro-simulation parameters modelling driver behaviour	Small Braess-like test network	1.6 - 2.6

Table 1. Details of key existing empirical POA studies with range of obtained POA values.

In this paper we use Motorway Incident Detection and Automatic Signalling (MIDAS) traffic data supplied by National Highways (NH) to create a TA model to analyse the empirical POA on the national-scale English Strategic Road Network (SRN). The approach uses efficient techniques to obtain accurate TA model inputs. It utilises a novel combination of road-specific density-based fitting of congestion function and network modularity-based community partitioning to obtain the Origin-Destination (O-D) demand matrix. The created data-driven model is used to analyse POA on the English SRN and investigate how the benefits of SO routing are distributed together with marginal external costs.

The results obtained indicate a small POA that is close to 1 for the English SRN (1.0011-1.0015). This implies that SO rerouting leads to approximately a 0.1% improvement in overall time savings on the network. This is a small value compared to many previous empirical studies (Table 1). For example, the study of the Eastern Massachusetts highway network in Zhang et al. (2018) using a similar data-driven model found POA values of up to 2.3, with a monthly average of 1.5. In a national-scale study of Singapore, a POA between 1.11 and 1.22 was obtained (Monnot et al. (2017)). However, the novel analysis of the zonal distribution of costs from rerouting reveals a more nuanced picture, with certain regions of the network exhibiting more significant changes in cost from rerouting.

This paper is structured as follows. In Section 2, the models and methods are presented to create the data-driven TA model. In Section 3, the data sets are presented together with the validation of the fitted TA model. Section 4 presents the numerical results relating to the POA and distribution of costs on the network. Finally, Section 5 concludes the paper.

2. Model and Methods

2.1. Network Definition

The road network is modelled as a directed graph with a set of nodes $\mathcal{V}$ and a set of edges $\mathcal{A}$. The model assumes the graph is strongly connected, on road networks in general, and the English SRN in particular, there is a path between all pairs of nodes so the assumption is valid. $\mathcal{F}$ is the set of vehicle flows permissible on the network.

Further details of the mathematical definition of the network including the properties and relations of the traffic flows and demands can be found in Zhang et al. (2018).

2.2. Calculating Congestion Functions

Congestion functions are key inputs for assignment models that link the travel time on each road to the vehicle flows. In this paper we use a density-based fitting of the Bureau of Public Roads (BPR) function based on Kucharski and Drabicki (2017) to estimate the functions for each edge of the network from traffic data with low computational cost.

The BPR equation is widely used in TA models (De Grange et al. (2017); Youn et al. (2008)). In its more general form for an edge $a \in \mathcal{A}$ it is:

$$t_a = t_a^0 \left(1 + \alpha (\frac{\check{x}_a}{m_a})^\beta \right), \tag{1}$$

where $\check{x}_a$ is the flow 'demand'. It should be clarified that flow demand defined here refers to the total number of drivers intending to travel through the specified road edge and this can exceed the defined road capacity, which is therefore distinct from actual measured or observed flow which is limited by capacity. m_a is the capacity and t_a^0 is the free-flow travel time.

Our method uses traffic density to transform the congestion function to a form that a curve can be fitted to using a non-linear least-squares approach and specific estimates of α and β parameters can be obtained (Kucharski and Drabicki (2017)). Estimating the traffic density using loop detector data is limited by the instantaneous time-mean measurements. In this work, the measured vehicle occupancy, together with mean length of vehicle and sensor length (2m for MIDAS), is used to estimate the traffic density as is commonly done in practice (Kim and Hall (2004)). The data used in the estimation include all daytime measurements averaged with 60-min mean values to remove outliers to steady-state conditions. m_a is taken as the maximum observed flow (Dervisoglu et al. (2009)). Free-flow speed v_0 is obtained as the 95th percentile of the observed speeds (Casey et al. (2020)) and t_0 from that through edge length l. The fitting is only applied to edges with sufficient data in the hyper-critical congested region. Edges without congested data assume values of $\alpha = 0.15$ and $\beta = 4$ and take the National Traffic Information Service (NTIS) values of capacity (National Highways (2022)).

2.3. Estimating the O-D Demand Matrix

The Generalised Least Squares (GLS) method, together with the Bi-Level optimisation problem (BiLev) adjustment algorithm, is used to estimate the key TA model input of the O-D demand matrix, without relying on external data sources beyond the empirical loop detector data (e.g. travel demand surveys). The method used in this work is similar to Zhang et al. (2018) and Roocroft et al. (2022).

As GLS has computational difficulties at larger network sizes, to obtain an estimate of the prior matrix a community partitioning approach is used to reduce computational difficulty, as described in Roocroft et al. (2022). This approach uses the Louvain algorithm for community detection based on network modularity to find the areas of the network most closely connected. It then applies the GLS method to the OD pairs in each partition separately. It combines these individual estimates into an estimate of the prior matrix, assuming zero demand for the OD pairs spanning partitions. In Roocroft et al. (2022) there are multiple ways of combining the partition OD estimates, this work uses the internal-only approach with two partitions as that has been shown to provide the best combination of accuracy and computational cost for networks of the size to be investigated here. The demand is calculated for discrete time-bins that approximate demand for static TA analysis. Three time-bins relating to workdays (Monday-Friday) are used: AM (6am-10am); MD (10am-4pm); PM (4pm-8pm).

2.4. Flow pattern calculation

The predicted UE flow pattern can be calculated using the calculated O-D demand matrix and congestion functions through the Frank-Wolfe algorithm with the following optimisation of the Traffic Assignment Problem (TAP) (see Patriksson (2015) for details):

$$\min_{\mathbf{x} \in \mathcal{F}} \sum_{a \in \mathcal{A}} \int_0^{\check{x}_a} t_a(s)ds \tag{2}$$

The UE flow pattern results from drivers pursuing their selfish best route and throughout this work it is assumed to match the observed flows as commonly done in other works (Zhang et al. (2018); Monnot et al. (2017); De Grange et al. (2017)). This type of deterministic UE assumes drivers are perfectly rational and have complete routing information available (Sheffi (1985)). More complex models use perceived cost to account for imperfect routing information in stochastic user equilibrium (Prato (2009)). Others use bounded rationality to model drivers' inertia to changing decisions (Di and Liu (2016)). Both of these alternatives can provide more realistic driver behaviour, however, they increase model complexity and require more computational requirements. Deterministic UE has been shown in recent research to match observed flow patterns fairly well at the network scale (Yildirimoglu and Kahraman (2018)) and it is widely used in many TA models for POA investigations (Zhang et al. (2018); Monnot et al. (2017); De Grange et al. (2017)).

For the network, the Total System Travel Time (TSTT) is defined by:

$$\mathcal{L}(\mathbf{x}) = \sum_{a \in \mathcal{A}} \check{x}_a t_a(\check{x}_a) \tag{3}$$

The SO flows which minimise the TSTT are formulated by the following non-linear optimisation problem:

$$\min_{\mathbf{x} \in \mathcal{F}} \sum_{a \in \mathcal{A}} \check{x}_a t_a(\check{x}_a) \tag{4}$$

This can also be solved using the Frank-Wolfe algorithm. The objective function of the SO optimisation can be expressed as the sum of the integrals of the marginal total costs of each edge $\bar{t}_a(x_a)$. Such that (Patriksson (2015)):

$$\bar{t}_a(\check{x}_a) \overset{\text{def}}{=} \frac{d}{d\check{x}_a} \check{x}_a t_a(\check{x}_a) = t_a(\check{x}_a) + \check{x}_a t_a'(\check{x}_a), \tag{5a}$$

$$\sum_{a \in \mathcal{A}} \check{x}_a t_a(\check{x}_a) = \sum_{a \in \mathcal{A}} \int_0^{\check{x}_a} \bar{t}_a(s) ds. \tag{5b}$$

The marginal total cost, $\bar{t}_a(\check{x}_a)$, of an edge a at $\check{x}_a$ can be interpreted as the increase in total cost on that edge from an additional driver joining that edge. In Equation 5a the total marginal cost is broken down into two components: $t_a(\check{x}_a)$ is the the marginal private cost; $\check{x}_a t_a'(\check{x}_a)$ is the marginal external cost. The difference between the UE and SO patterns results from the individual driver's avoidance of paying all the cost that they contribute to the system's total travel cost. From an economics perspective, a driver's private cost does not equal their total cost to the system due to the external costs they do not pay.

An understanding of the spatial and temporal distribution of marginal costs on specific road edges would allow for more targeted strategies that could encourage SO routing for individual drivers. For example, by specifying road road charges during specific periods or at particular road edges, a traffic flow distribution that is closer to SO routing could be achieved (Patriksson (2015)). For static TA models with BPR congestion functions, the values of the marginal external cost, $\check{x}_a t_a'(\check{x}_a)$, for an edge $a \in \mathcal{A}$ with a road-specific BPR congestion function is calculated by:

$$\check{x}_a t_a'(\check{x}_a) = \frac{t_a^0 \beta_a \alpha_a}{m_a^{\beta_a}} \check{x}_a^{\beta_a}, \tag{6}$$

where the parameters α_a and β_a are the BPR coefficients fitted to edge a. This can be derived by differentiating Equation 1 with respect to $\check{x}_a$ and then multiplying by $\check{x}_a$.

3. Data sets and Model Fitting

For the purpose of this article, we utilise traffic data obtained through the MIDAS system for the period September 2018 to August 2019. MIDAS mostly records traffic through inductive loops spaced approximately every 500m at approximately 7000 sites on the England SRN (Highways England (2019)). Details of pre-processing MIDAS data for TA analysis can be found in (Roocroft et al. (2022)).

The NTIS model contains the information on the details and location of assets used to monitor traffic on the SRN, such as the location of MIDAS sensor sites and geospatial information of the road junctions that can be converted into a graph representation of the network (Highways England (2019)). The NTIS is subjected to conventional data processing to remove inaccuracies and create a 278 edge topographic representation of the main carriageways comprising the national SRN monitored by MIDAS. The partitioned topographic representation of the network (Figure 1) is used to obtain the O-D matrix.

The density-based BPR congestion function fitting method is applied to 231 suitable edges of the network (83% of total), with these edges selected based on suitable data. The fitted congestion functions and O-D matrices are used to obtain the errors in the resulting UE traffic pattern compared to the observed edge flows and travel times.

The Absolute Percentage Errors (APE) are calculated as:

$$APE_a^t = \frac{|t_{p,a}^{user} - t_{p,a}^{obs}|}{t_{p,a}^{obs}}, \tag{7}$$
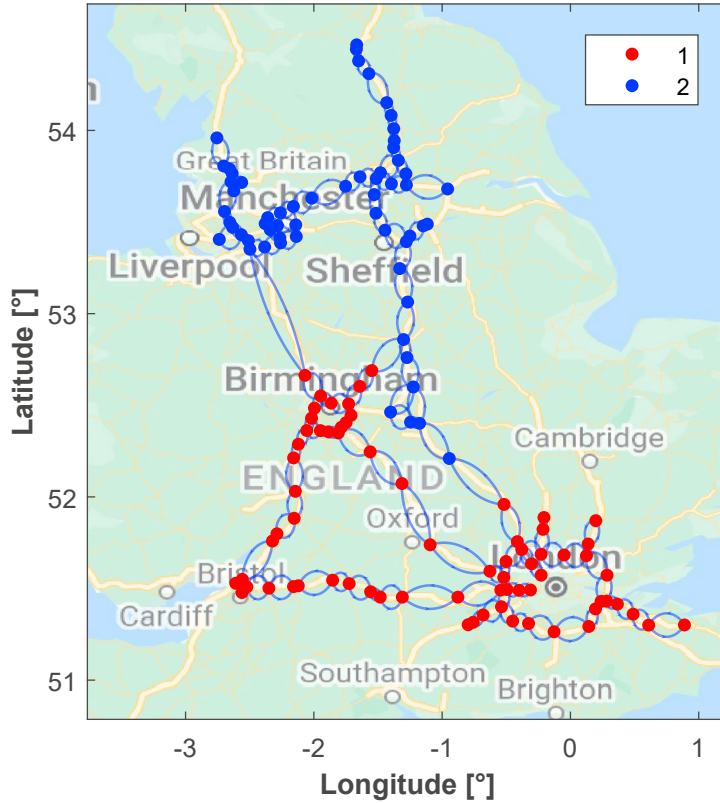
Figure 1. Topographic representation of the simplified NTIS model for the SRN subnetwork. The two colours of nodes indicate the partitions used for demand profile estimation. Map underlay from Google Maps (Google Maps (2022)).

for travel time, while

$$APE_a^x = \frac{|x_{p,a}^{user} - x_{p,a}^{obs}|}{x_{p,a}^{obs}}, \tag{8}$$

is used for flows. For each time-bin p and edge a, $x_{p,a}^{obs}$ is the observed flow and $t_{p,a}^{obs}$ is the travel time derived from observed speed. The values are the mean within each time-bin over the fitting period. $t_{p,a}^{user}$ is the predicted travel time derived from the congestion function using $x_{p,a}^{user}$, which is the edge flow value predicted by the model through solving the UE TAP with the calculated O-D matrix.

The inaccuracy of the UE assignment prediction is also assessed through the error in TSTT, $\mathcal{L}_{error}$, such that:

$$\mathcal{L}_{error}^p(\mathbf{x}^{ue}) = \frac{\sum_{a \in \mathcal{A}} x_{p,a}^{user} t_{p,a}^{user} - \sum_{a \in \mathcal{A}} x_{p,a}^{obs} t_{p,a}^{obs}}{\sum_{a \in \mathcal{A}} x_{p,a}^{obs} t_{p,a}^{obs}}, \tag{9}$$

for time-bin p. This calculation combines the errors in flow and time prediction and has particular relevance for analysis based on aggregate total system cost

The validation results (Table 2) show the travel time error is fairly low and the overall error in TSTT, $\mathcal{L}_{error}(\mathbf{x}^{ue})$, is only 7.9% on average across the time-bins. The results can be compared with recent TA modelling work (Dey

et al. (2020)) that used similar network tomography-based O-D matrix estimation techniques to obtain the TA input for a small 23 node, 54 edge network in Melbourne, Australia. That model had a mean flow APE of 24.18% using simulated data. Using travel time data from Uber and Syic, they found mean APEs in travel time predictions of 18 - 33%. Although these results are not directly comparable as the networks are different, they demonstrate the approximate size of errors for current similar real-world data-driven static TA models. As Table 2 shows similar errors for a much larger network, the derived static TA model is reasonably suitable for the following analysis.

	Mean Flow APE (%)	Mean Travel Time APE (%)	Median Flow APE (%)	Median Travel Time APE (%)	$\mathcal{L}_{error}(\mathbf{x}^{ue})$ (%)
AM	32.8	16.6	23.0	4.8	-7.8
MD	30.9	16.5	22.4	4.3	-4.6
PM	32.6	16.4	26.0	4.4	-11.2

Table 2. Time-bin specific User-Equilibrium (UE) prediction error statistics for all edges on network during the analysis period September 2018 to August 2019. The mean and median errors refers to the mean and median across all the edges.

4. Results

4.1. Routing Efficiency

Using the calculated UE and SO flow patterns, the POA can be calculated through:

$$POA = \frac{\mathcal{L}(\mathbf{x}^{UE})}{\mathcal{L}(\mathbf{x}^{SO})} \, , \tag{10}$$

where $\mathcal{L}(\mathbf{x}^{UE})$ is the sum of the calculated UE flow vector multiplied by the calculated UE travel time vector resulting from the congestion functions. Likewise, $\mathcal{L}(\mathbf{x}^{SO})$ is the SO flow vector multiplied by its travel time vector.

After calculating the TSTT for the UE and SO flow patterns, the POA is found to be very low (Table 3). On average, the POA for the three time-bins is 1.0013. This indicates that the network does not have a large potential for savings in overall congestion from rerouting selfish drivers in a more system optimal way. The obtained values are due to the interplay of the SRN's demand profile, congestion functions and network structure (Belov et al. (2022)). A major influence on the low POA values is the large free-flow travel times of the congestion functions of the SRN, which dwarf the time savings from rerouting and lead to smaller POA values (O'Hare (2015)). This combines with a general lack of routing options on the network and a time-bin average demand profile that smooths out peak demand to a lower level, which also reduce the POA (O'Hare et al. (2016)). These aspects joined together lead to POA values on the low end of those found in the literature, and could be expected for other similar networks.

Table 3. Price of Anarchy (POA) during the period September 2018 to August 2019.

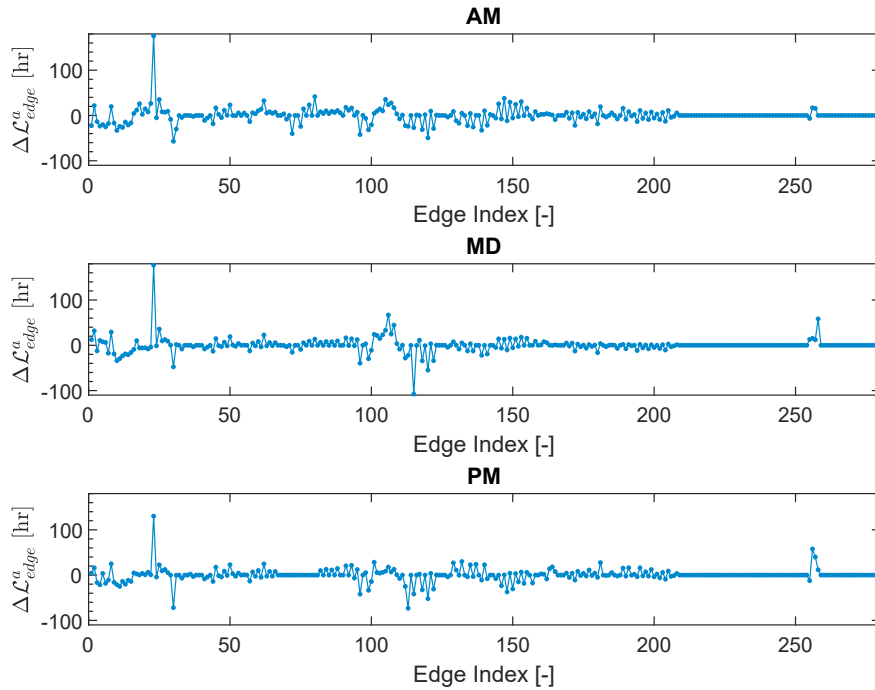| Time Bin	$\mathcal{L}(\mathbf{x}^{ue})$ [hr]	$\mathcal{L}(\mathbf{x}^{SO})$ [hr]	POA
AM	87797	87662	1.0015
MD	87835	87709	1.0014
PM	82921	82831	1.0011

Figure 2. Difference in the total cost on each edge of the network between User-Equilibrium (UE) and System-Optimal (SO) flow patterns in each time-bin. Results are for edges on network, using data from the weekdays selected for analysis between September 2018 and August 2019.

4.1.1. Network Cost Distribution

The travel cost on a single edge $a \in \mathcal{A}$, $\mathcal{L}_{edge}(x_a)$, is defined as:

$$\mathcal{L}_{edge}(\check{x}_a) \stackrel{\text{def}}{=} \check{x}_a t_a(\check{x}_a). \tag{11}$$

The difference between the edge cost for UE and SO flow patterns is then defined as:

$$\Delta \mathcal{L}_{edge}^a \stackrel{\text{def}}{=} \mathcal{L}_{edge}(\check{x}_a^{UE}) - \mathcal{L}_{edge}(\check{x}_a^{SO}). \tag{12}$$

To investigate how the traffic cost is redistributed between UE and SO flow patterns, the difference in the cost on each edge, $\Delta \mathcal{L}_{edge}^a$ (Equation 12), is plotted in Figure 2. Other quantities such as the saturation rate, x_a/m_a, and delay factor, $t_a(x_a)/t_a^0$, could be used to show the effect of the different routing; however, the difference in edge cost is the most relevant as it captures both flow and travel time together.

The plots in Figure 2 show that there are many edges that do not have routing differences, for example between edges 220 to 250. These edges correspond to the areas of the network that only have single routes. These are called bridge edges and removing them would prevent certain nodes from being accessible from the rest of the network. Of the 278 edges of the network, 90 are classed as bridge edges (32.4%). These large portions of the network with only one route limit the effectiveness of rerouting and contribute to the low overall POA values found in Table 3.

The edges without cost differences are highlighted in red and purple in Figure 3. The red Group 2 edges are the bridge edges that only have one route available to their attached nodes, they do not have a difference in any time-bin. The edges in the purple Group 3 change across time-bins. This shows that the edges in the main subnetwork that are
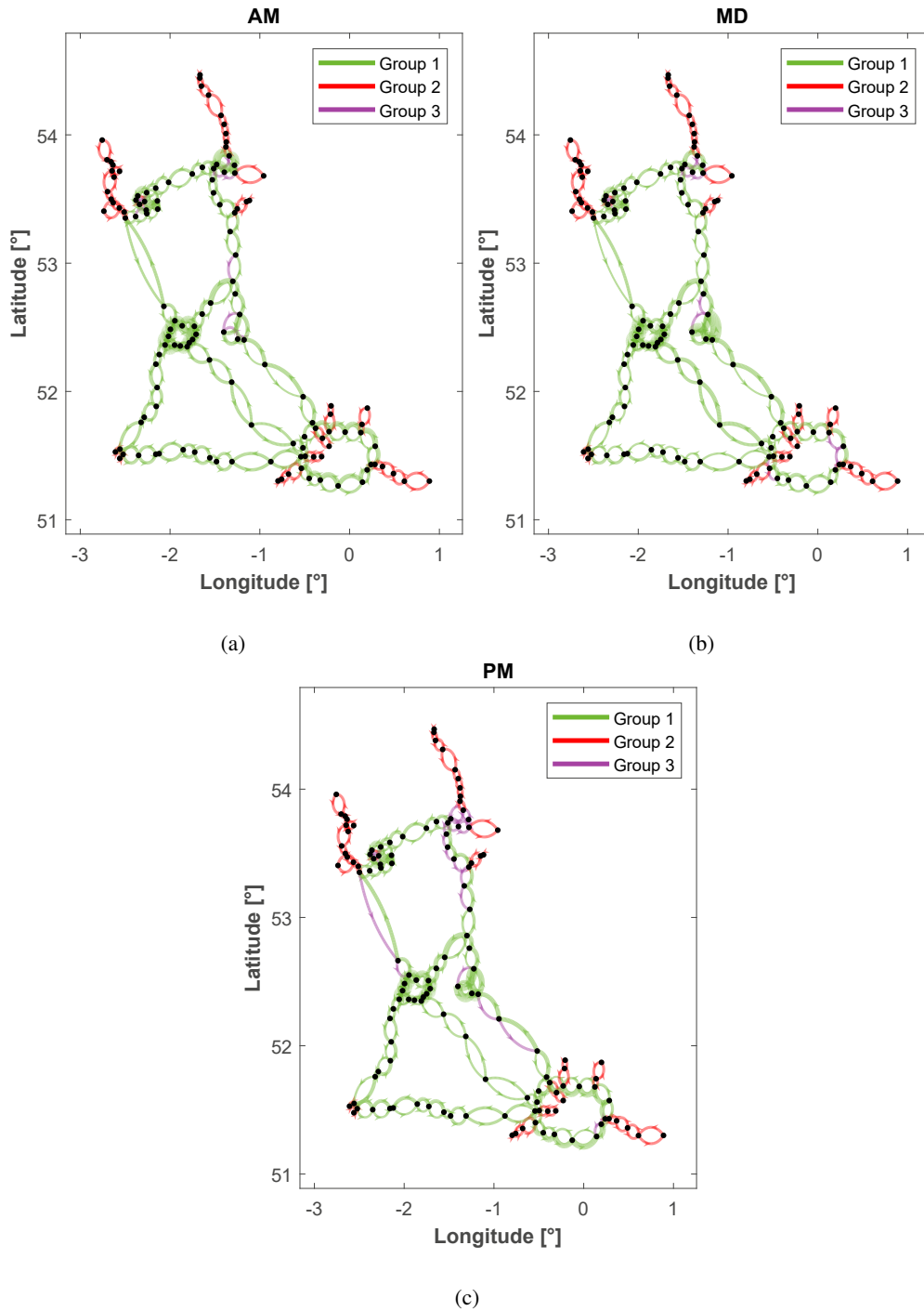
(a)

(b)

(c)

Figure 3. Edges on network that have cost differences between User-Equilibrium (UE) and System-Optimal (SO) flow patterns during the analysis period September 2018 to August 2019: (a) AM; (b) MD; (c) PM. Edge thickness is proportional to change in edge cost. Group 1 are edges with differences in cost between UE and SO routing. Group 2 are bridge edges without any difference in cost. Group 3 are non-bridge edges without any difference in cost.
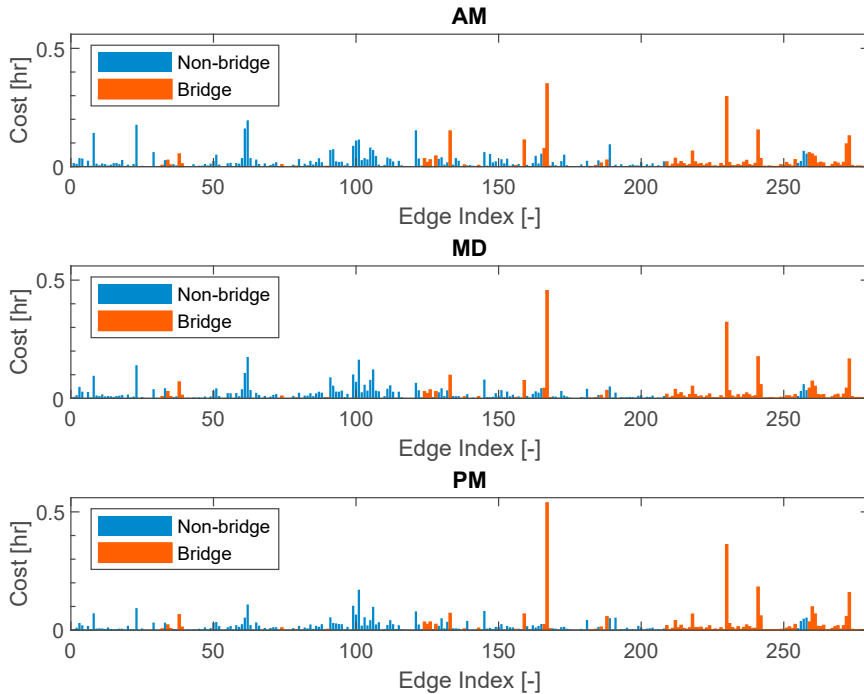
Figure 4. Marginal external cost for each edge and each time-bin on the network for the analysis period September 2018 to August 2019. Bridge edges on the network (those with single routes) are indicated with red bars, non-bridge edges are indicated with blue bars.

not 'bridges' yet present no cost difference, change depending on the demand profile of the time-bin considered. This highlights the influence demand profile structure can have on the outcome of rerouting.

The marginal external cost for each edge and time-bin is shown in Figure 4. Notably, some of the highest marginal external costs are on bridge edges. High road charges on them would entail implementation difficulties as they only have one route to their associated nodes. Drivers wishing to access these nodes would have no alternative choice of route, meaning the road charges would not directly affect the routing. Instead, these road charges would likely have unconsidered secondary effects on mode choice and patterns of demand, as drivers may not want to use the available road system for affected journeys. This highlights a problem for any road network with bridge edges, which reduce routing options and the opportunity to benefit from rerouting. However, the network model we have used here, is actually a simplification of the actual road network (since we do not include smaller roads in the model) and alternative routes would be available in reality.

4.2. Effect of Rerouting in Zones of SRN

We use zonal cost difference to analyse the cost difference between zones of the network to see how the rerouting benefits are distributed across the network. This is defined as:

$$\Delta \mathcal{L}_z \stackrel{\text{def}}{=} \frac{\mathcal{L}(\mathbf{x}_z^{UE}) - \mathcal{L}(\mathbf{x}_z^{SO})}{|\mathcal{A}^z|}, \tag{13}$$

where for UE and SO flow patterns, $\mathcal{A}^z$ is the set of edges in zone z and $\mathcal{L}(\mathbf{x}_z) = \sum_{a \in \mathcal{A}^z} \check{x}_a t_a(\check{x}_a)$. The difference in the total costs in the zone from rerouting is divided by the number of edges in the zone $|\mathcal{A}^z|$ to give a mean zonal cost difference per edge. Additionally, the mean marginal external cost for a zone is calculated by the sum of the marginal external costs of the edges in a zone $\mathcal{A}^z$ divided by the number of edges in the zone $|\mathcal{A}^z|$.

Although the POA on the network is small, the change in costs from rerouting UE flow patterns to SO is distributed differently across the network. For the network overall, the total costs decrease when changing the routes taken by drivers, however, the benefits of this are not evenly distributed. For example, in Figure 2 it can be seen that the edges 1-28 have some of the highest redistribution of costs. These edges correspond to the roads around the Birmingham area.

To investigate the pattern of redistribution of costs from rerouting, in Figure 5 we identify a sample of zones. These split the network into broad geographic regions (e.g. North, South) and also city regions (e.g. London). In order to reduce the unwanted effect of the bridge edges identified (Figure 3) (since they can have no impact on improving rerouting), we remove them from this zonal analysis. The parts of the network that contain the bridge edges decrease the opportunity to lower the TSTT through rerouting, as they contribute to the total demand but cannot vary routing between UE and SO.

In Figure 6 (a), it can be seen that there are variations in the changes to the zonal costs from rerouting between different zones and time-bins. For example, between North, South and Middle it is apparent that North benefits the most from rerouting, in particular in the AM time-bin. This comes at the expense of the edges in the Middle zone, however, in the MD time-bin that zone does have a slight positive reduction in cost. In Figure 6 (b), it can be seen that, of the three zones, the highest mean edge marginal external cost is within the Middle region, highlighting that if a marginal cost road charge scheme was implemented then higher road charges would be paid in the region with the least reduction in time cost.

When the subnetwork is divided between the East and West zones, it can be seen that in AM and PM the West zone benefits more than the East. However, in the MD time-bin East benefits slightly more than West. In the city zones it is clear that Birmingham (BHM) has the largest reduction in cost of all the three, however, London (LDN) has higher mean edge marginal external costs.

In the Core zone, with the bridge edges removed, there is a positive reduction in cost across all time-bins. Using the Core zonal cost totals in the POA calculation leads to higher values than those obtained for the whole network (AM 1.0021 ; MD 1.0020 ; PM 1.0015).

The zone with the clearest benefit from SO rerouting consists of the 24 edges which represent roads surrounding Birmingham (BHM). When the total costs of this zone are included in the POA analysis, the values are considerably higher than for the whole network (AM 1.0203 ; MD 1.0262 ; PM 1.0154). BHM is clearly a beneficiary of rerouting on the network, however, the Middle zone of which it is a part of, is a zone which loses overall from rerouting. This is due to the position of the zones, the structure of the network and the profiles of demand. Depending on how the network is divided into zones, different aggregate results are obtainable. Overall, the network benefits from rerouting, however, users in distinct areas of the country with different needs from the transport system would perceive the changes differently. Further understanding of the causes that lead to different zones benefiting or losing out due to rerouting is beyond this analysis; however, future work could build on this insight.

5. Conclusion

In this paper we presented a high level structural analysis of the motorway system of the English SRN covered by the MIDAS system over a year. From the analysis we showed through the POA metric that the opportunity to improve overall congestion on the SRN network through rerouting selfish drivers was limited in the analysis period. When compared to previous empirical POA studies the values obtained were relatively small. This was due to the interaction of the demand profile with the network structure and congestion functions. In line with previous POA research, contributing factors to this were large free-flow travel times in the congestion functions and lower levels of demand. Another contributing factor was the presence of a large number of bridge edges that reduce routing options. It was highlighted how bridge edges could cause implementation issues for marginal cost road charging if the charges on them were high. In general, a large number of bridge edges would likely make rerouting schemes unsuitable for a network.

The created data-driven TA model was used to investigate the distribution of the costs and benefits of rerouting across the road system, which was found to vary strongly with different areas and time-bin demand profiles. This distribution did not match with the distribution of marginal external costs on the network. Zones of the network with

(a) North, South, Middle

(b) East, West

(c) Cities
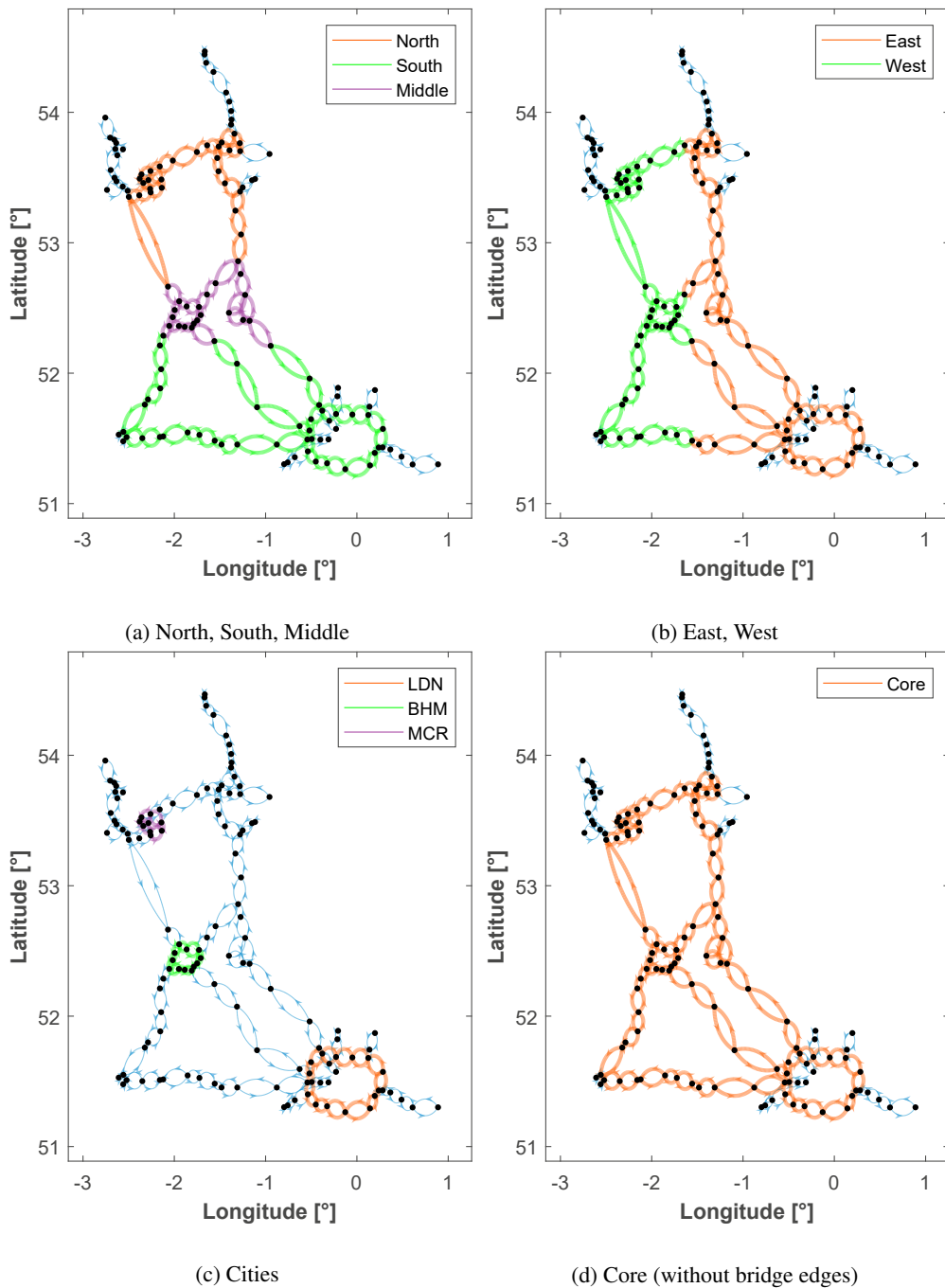
(d) Core (without bridge edges)

Figure 5. Zonal divisions of the topographic representation of the network. (a) North, South, Middle; (b) East and West; (c) Cities- London (LDN), Birmingham (BHM), Manchester (MCR); (d) Core subnetwork without bridge edges. The edges with thin blue lines are excluded from the zones.

the largest benefits from rerouting were not often those where the largest marginal external cost road charges would be applied, which has implications for public acceptance of any such road charge scheme as it may be seen as unfair.

The techniques in this research could be used by transport planners to build a suitable TA model solely from widely-available loop detector measurements and analyse at different scales the viability of system optimal routing schemes for improved understanding of potential cost and benefit distributions. Future work could investigate the

(a) Mean edge change in cost

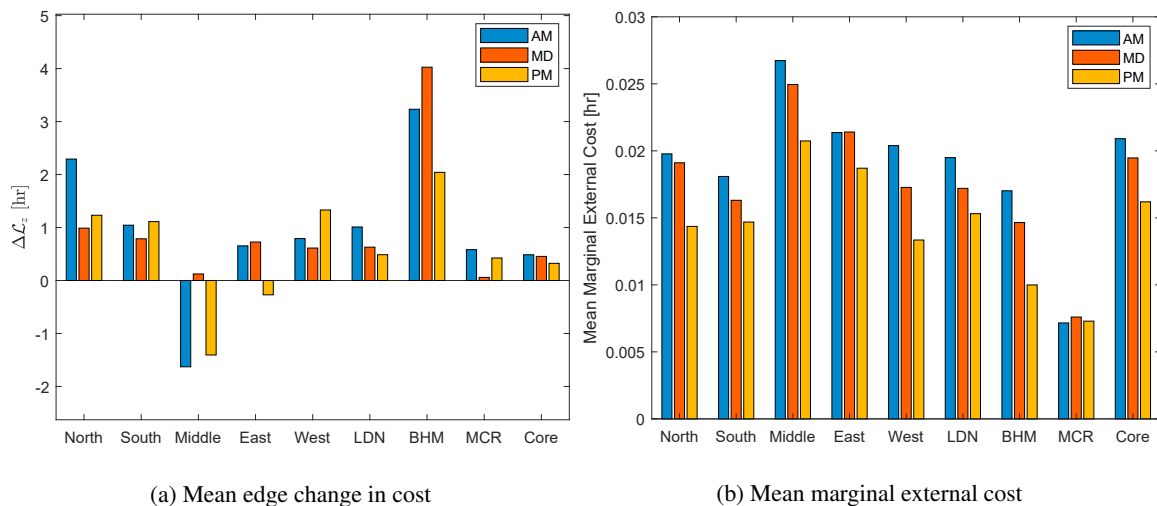(b) Mean marginal external cost

Figure 6. Zonal distribution on the network of cost differences between User-Equilibrium (UE) and System-Optimal (SO) flow patterns in each time-bin during the analysis period September 2018 to August 2019: (a) Mean edge change in cost from rerouting in different zones; (b) Mean marginal external costs in each zone. The mean is across all the edges of the zone.

relationship between network structure, demand profile and cost changes to further understand why different zones have the response they do to rerouting and how rerouting benefits are shared across the network compared to applied road charges.

Acknowledgment

References

Belov, A., Mattas, K., Makridis, M., Menendez, M., Ciuffo, B., 2022. A microsimulation based analysis of the price of anarchy in traffic routing: The enhanced braess network case. Journal of Intelligent Transportation Systems 26, 448–460. URL: https://doi.org/10.1080/15472450.2021.1904920, doi:10.1080/15472450.2021.1904920, arXiv:https://doi.org/10.1080/15472450.2021.1904920.

Casey, G., Zhao, B., Kumar, K., Soga, K., 2020. Context-specific volume–delay curves by combining crowd-sourced traffic data with automated traffic counters: A case study for London. Data-Centric Engineering 1.

De Grange, L., Melo-Riquelme, C., Burgos, C., González, F., Raveau, S., 2017. Numerical Bounds on the Price of Anarchy. Journal of Advanced Transportation 2017, 1–9. doi:10.1155/2017/5062984.

Dervisoglu, G., Gomes, G., Kwon, J., Muralidharan, A., Varaiya, P., Horowitz, R., 2009. Automatic Calibration of the Fundamental Diagram and Empirical Observations on Capacity, in: Transportation Research Board 88th Annual Meeting, TRB, Washington, D.C.. pp. 1–14.

Dey, S., Winter, S., Tomko, M., 2020. Origin–destination flow estimation from link count data only. Sensors 20. doi:10.3390/s20185226.

Di, X., Liu, H.X., 2016. Review. Transportation Research Part B: Methodological 85, 142–179. doi:10.1016/j.trb.2016.01.002.

Google Maps, 2022. Map of Central England. URL: https://www.google.com/maps/place/England,+UK/. available online at: https://www.google.com/maps/place/England,+UK/, last accessed on 27/10/2022.

Highways England, 2019. National Traffic Information Service DATEX II Service v10. Technical Report. Highways England. London.

Hymel, K.M., Small, K.A., Dender, K.V., 2010. Induced demand and rebound effects in road transport. Transportation Research Part B: Methodological 44, 1220–1241. URL: https://www.sciencedirect.com/science/article/pii/S0191261510000226, doi:https://doi.org/10.1016/j.trb.2010.02.007.

INRIX, 2021. INRIX Research: Global Traffic Scorecard. Technical Report. INRIX. URL: https://inrix.com/scorecard/, doi:10.1163/156854108783360159.

Kim, Y., Hall, F.L., 2004. Relationships between occupancy and density reflecting average vehicle lengths. Transportation Research Record 1883, 85–93.

Kucharski, R., Drabicki, A., 2017. Estimating macroscopic volume delay functions with the traffic density derived from measured speeds and flows. Journal of Advanced Transportation 2017, 1–10. doi:10.1155/2017/4629792.

Monnot, B., Benita, F., Piliouras, G., 2017. Routing games in the wild: Efficiency, equilibration and regret, in: R. Devanur, N., Lu, P. (Eds.), Web and Internet Economics, Springer International Publishing, Cham. pp. 340–353.

National Highways, 2022. National highways traffic information services. URL: https://www.trafficengland.com/subscribers. available online at: https://www.trafficengland.com/subscribers, last accessed on 27/11/2022.

O'Hare, S.J., 2015. The Influence of Structure in Supply and Demand on the Performance Characteristics of Road Traffic Networks: An exploration of how methodological approaches from network science can be implemented for a transportation research problem. Ph.D. thesis. University of Leeds. URL: https://etheses.whiterose.ac.uk/9151/.

O'Hare, S.J., Connors, R.D., Watling, D.P., 2016. Mechanisms that govern how the Price of Anarchy varies with travel demand. Transportation Research Part B: Methodological 84, 55–80. URL: https://www.sciencedirect.com/science/article/pii/S0191261515002660, doi:https://doi.org/10.1016/j.trb.2015.12.005.

Patriksson, M., 2015. The Traffic Assignment Problem: Models and Methods. 2 ed., Dover Publications, Mineola, N.Y. URL: https://books.google.com.sg/books?id=PDhkBgAAQBAJ.

Prato, C.G., 2009. Route choice modeling: past, present and future research directions. Journal of Choice Modelling 2, 65–100. URL: https://www.sciencedirect.com/science/article/pii/S1755534513700058, doi:https://doi.org/10.1016/S1755-5345(13)70005-8.

Roocroft, A., Punzo, G., Ramli, M.A., 2022. Link count data-driven static traffic assignment models through network modularity partitioning (pre-print). URL: https://arxiv.org/abs/2211.13514, doi:10.48550/ARXIV.2211.13514.

Sheffi, Y., 1985. Urban transportation networks: Equilibrium analysis with mathematical programming methods. 1 ed., Prentice-Hall Inc, Englewood Cliffs, N.J. doi:10.1016/0191-2607(87)90038-0.

Wu, Z., Möhring, R.H., Chen, Y., Xu, D., 2021. Selfishness need not be bad. Operations Research 69, 410–435. URL: https://doi.org/10.1287/opre.2020.2036, doi:10.1287/opre.2020.2036, arXiv:https://doi.org/10.1287/opre.2020.2036.

Yildirimoglu, M., Kahraman, O., 2018. Searching for empirical evidence on traffic equilibrium. PLOS ONE 13, 1–16. URL: https://doi.org/10.1371/journal.pone.0196997, doi:10.1371/journal.pone.0196997.

Youn, H., Gastner, M.T., Jeong, H., 2008. Price of anarchy in transportation networks: Efficiency and optimality control. Physical Review Letters 101, 1–4. doi:10.1103/PhysRevLett.101.128701, arXiv:0712.1598.

Zhang, J., Pourazarm, S., Cassandras, C.G., Paschalidis, I.C., 2018. The Price of Anarchy in Transportation Networks: Data-Driven Evaluation and Reduction Strategies. Proceedings of the IEEE 106, 538–553. doi:10.1109/JPROC.2018.2790405, arXiv:arXiv:1606.02194v2.